Transverse electric-field-induced magnetophonon resonance in *n*-type germanium

S. C. Lee and Y. B. Kang
Department of Physics, Cheju National University, Cheju 690-756, Korea

G. Y. Hu
Department of Physics, Cheju National University, Cheju 690-756, Korea
and Department of Physics, Louisiana State University, Baton Rouge, Louisiana 70803

J. Y. Ryu
Department of Physics, Cheju National University, Cheju 690-756, Korea

S. D. Choi
Department of Physics, Kyungpook National University, Taegu 702-701, Korea
(Received 3 September 1997; revised manuscript received 8 December 1997)

We investigate the influence of the intracollisional field effect in the hot-electron regime of the transverse magnetophonon resonances in *n*-type germanium. Our results show that double peaks take place according to the nonvertical transition due to the intracollisional field effect. One of the peaks is shifted to the lower-magnetic-field side and the other is shifted to the higher-magnetic-field side as electric fields are increased and as the possible phonon energy and the difference of Landau-level indices are decreased. It is also shown that the peaks depend on the magnetic-field direction giving rise to the difference in the effective mass between the initial and final states. [S0163-1829(98)03615-7]

I. INTRODUCTION

With the recent advance of pulsed high-magnetic-field technique, it has been possible to measure the magnetophonon resonance (MPR) effect in a very high magnetic field. Many studies on the ordinary and hot-electron MPR effects in *n*-type Ge have been made for longitudinal and transverse configurations.[1–8] It is known that Ge exhibits rich spectra of MPR because optical phonons and zone-edge acoustic phonons couple with electrons by the deformation potential interaction, although it is not a polar semiconductor. The MPR spectra in *n*-type Ge is quite complicated due to the complexity of phonon branches and the variety of intervalley transitions, which results in difficulties in the assignment of each electronic transition.[8] In the high-field range, the MPR peaks for *n*-type Ge are well resolved from each other, so that one can assign each peak to a specific transition.

For the transverse magnetoconductivity configuration, where the current and the magnetic-field directions are perpendicular to each other, Harper *et al.*[5] presented the experimental results of MPR in *n*-Ge for the magnetic field parallel to the ⟨100⟩ and ⟨110⟩ directions. Their results show that the transverse magnetoconductivity oscillates as a function of the magnetic field. Eaves *et al.*[2] also presented the experimental results of MPR in *n*-Ge for the magnetic field parallel to the ⟨100⟩ and ⟨111⟩ directions. A recent review of the MPR effects was given by Ridley.[6]

For the longitudinal hot-electron magnetoconductivity configuration, where the current and the magnetic-field directions are parallel, Hamaguchi *et al.*[3,4] found that in the electric field ranging from 17 to 73 V/cm several different series of oscillations for the ⟨100⟩ direction of *n*-Ge at 20 K were present. Recently, Futagawa *et al.*[8] presented experimental results of *n*-type Ge for the magnetic-field direction parallel to the ⟨100⟩, ⟨111⟩, and ⟨110⟩ directions. Their results show that the dominant MPR signal arises from the hot-electron transitions from the valley with lighter cyclotron mass to the valley with heavier mass in *n*-type Ge. It was also shown that the hot-electron MPR peaks are observed for the intervalley and intravalley scatterings. Note that all the experiments discussed above were performed for the case where the intracollisional field effect (ICFE) is not effective in the hot-electron regime. Therefore, our concerns are to investigate the changes of the resonance fields due to the ICFE that are effective in the hot-electron regime with electric fields of the order of 10^5 V/cm.[9]

In this paper we present a theory of transverse electric-field-induced MPR in *n*-type Ge, on the basis of the high-field quantum-statistical transport theory[10] developed by some of the present authors, and investigate the MPR extrema of *n*-type Ge for the magnetic-field direction parallel to the ⟨100⟩, ⟨110⟩, and ⟨111⟩ directions as the strength of the electric fields increases.

The paper is arranged as follows. In Sec. II we describe a simple model of the system. In Sec. III we present the field-dependent magnetoconductivity formula related to the relaxation rate by using the result of nonlinear-response theory obtained previously. The transverse hot-electron MPR is discussed, where special attention is given to the MPR peak positions. Results are given in Sec. IV and we conclude in Sec. V.

II. MODEL OF THE SYSTEM

We choose Cartesian coordinate axes with the z axis parallel to the principal axis of an ellipsoidal energy surface. In the presence of a static magnetic field tilted with an angle of θ from the z axis, $\mathbf{B}=B(\sin\theta,0,\cos\theta)$, and a uniform external electric field $\mathbf{E}=E\hat{y}$, the one-electron Hamiltonian is given as

$$h_{eE}=\frac{1}{2}(\mathbf{p}+e\mathbf{A})\begin{pmatrix}1/m_t & 0 & 0\\ 0 & 1/m_t & 0\\ 0 & 0 & 1/m_l\end{pmatrix}(\mathbf{p}+e\mathbf{A})+eEy, \quad (2.1)$$

where $\mathbf{A}$ is the vector potential, $\mathbf{p}$ is the momentum operator, and m_t and m_l represent the transverse and longitudinal mass components of the ellipsoidal energy surface of the conduction band, respectively. By taking into account the Landau gauge $\mathbf{A}=B(-y\cos\theta,0,y\sin\theta)$, the one-electron normalized eigenfunctions and eigenvalues of the s valley of the conduction band are given, respectively, by

$$\langle\mathbf{r}|\lambda s\rangle\equiv\langle\mathbf{r}|N,k_x,k_z,s\rangle=U^s(\mathbf{r})F_\lambda(\mathbf{r}), \quad (2.2)$$

$$E_\lambda^s=E_N^s(k_x,k_z)=\varepsilon_\lambda^s+eEy_\lambda^s+\frac{m_tm_l}{2m_B^s}V_d^2, \quad (2.3)$$

with

$$\varepsilon_\lambda^s=(N+1/2)\hbar\omega_s+\frac{\hbar^2}{2m_B^s}\left(\frac{\mathbf{k}\cdot\mathbf{B}}{B}\right)^2, \quad (2.4)$$

$$y_\lambda^s=-\frac{\hbar}{eBm_B^s}\left[m_tk_z\sin\theta-m_lk_x\cos\theta+\frac{m_tm_lV_d}{\hbar}\right], \quad (2.5)$$

where N $(=0,1,2,\ldots)$ are the Landau-level indices, k_x and k_z are, respectively, the wave-vector components of the electron in the x and z directions, s in the superscript or subscript indicates the valley index of the conduction band, V_d $(=E/B)$ is the drift velocity, and $\omega_s(=eB/m_s^*)$ and m_B^s are, respectively, the cyclotron frequency and the effective mass in the magnetic-field direction, which are

$$\frac{1}{m_s^{*2}}=\frac{\cos^2\theta}{m_t^2}+\frac{\sin^2\theta}{m_tm_l}, \quad (2.6)$$

$$m_B^s=m_l\cos^2\theta+m_t\sin^2\theta. \quad (2.7)$$

Also in Eq. (2.2), $U^s(\mathbf{r})$ denotes the Bloch function of the s valley and $F_\lambda(\mathbf{r})$ means the envelope function given by

$$F_\lambda(\mathbf{r})=\frac{1}{\sqrt{L_xL_z}}\phi_N(y-y_\lambda^s)\exp(ik_xx+ik_zz), \quad (2.8)$$

where $\phi_N(y)$ in Eq. (2.8) are the eigenfunctions of the simple harmonic oscillator and L_x and L_z are, respectively, the x and z directional normalization lengths. We assume that the Bloch function $U^s(\mathbf{r})$ and the envelope function $F_\lambda(\mathbf{r})$ are, respectively, normalized in the crystal as

$$\int_C U^{s*}(\mathbf{r})U^{s'}(\mathbf{r})d^3r=\delta_{s,s'}, \quad (2.9)$$

$$\int_\Omega F_\lambda^*(\mathbf{r})F_{\lambda'}(\mathbf{r})d^3r=\delta_{\lambda,\lambda'}, \quad (2.10)$$

where C is the volume of the unit cell and Ω $(=L_xL_yL_z)$ is the crystal volume in real space.

III. FIELD-DEPENDENT MAGNETOCONDUCTIVITY ASSOCIATED WITH RELAXATION RATES

We now want to evaluate the field-dependent magnetoconductivity $\sigma_{yy}(E)$ for the system modeled in Sec. II by using eigenfunctions and eigenvalues given in Eqs. (2.2) and (2.3) and the general expression for the nonlinear dc conductivity $\tilde{\sigma}_{kl}(E)$ $(k,l=x,y,z)$ derived in Ref. 10. It is straightforward to show that the transverse magnetoconductivity $\sigma_{yy}(E)$ can be expressed in terms of Eqs. (2.2) and (2.3) as

$$\sigma_{yy}(E)\cong\frac{\hbar}{\Omega}\sum_{\lambda,s}\sum_{\lambda',s'}|\langle\lambda s|j_y|\lambda's'\rangle|^2\frac{f(\varepsilon_\lambda^s)-f(\varepsilon_{\lambda'}^{s'})}{\varepsilon_\lambda^s-\varepsilon_{\lambda'}^{s'}}\frac{\Gamma_{\lambda's',\lambda s}(E)}{(E_\lambda^s-E_{\lambda'}^{s'})^2}, \quad (3.1)$$

where $j_y=-(e/m_t)p_y$ is the y component of a single-electron current operator, $f(\varepsilon_\lambda^s)$ is the Fermi-Dirac distribution function associated with the eigenvalue of Eq. (2.4), and $\Gamma_{\lambda's',\lambda s}(E)$ is the field-dependent relaxation rate, which appears in terms of the collision broadening due to the electron-phonon interaction. To obtain Eq. (3.1) we have assumed that the energy difference $(E_\lambda^s-E_{\lambda'}^{s'})$ between the Landau energy of the s valley and that of the s' valley is larger than the quantities such as the width and the shift in the spectral line shape, which is usually satisfied and is in fact the condition to observe the oscillatory behavior of hot-electron MPR.[11] In the intervalley transitions, the matrix elements of the single-electron current operator in Eq. (3.1) are given, in terms of Eq. (2.2), by

$$|\langle\lambda s|j_y|\lambda's'\rangle|^2=S(s,s')\delta_{\lambda,\lambda'}, \quad (3.2)$$

where $S(s,s')=|\langle s|j_y|s'\rangle|^2$ and the Kronecker symbols $(\delta_{\lambda,\lambda'}=\delta_{N',N},\delta_{k_x,k_x'},\delta_{k_z,k_z'},\delta_{s,s'})$ denote the selection rules.

Within the first-order Born approximation of scattering processes, the matrix elements of $\Gamma(E)$ associated with the transition between the states $|\lambda s\rangle$ and $|\lambda s'\rangle$ is generally given[10,11] by

$$\Gamma_{\lambda s',\lambda s}(E)=\pi\sum_{\mathbf{q}}\{[N_{\mathbf{q}}(T)+1]M_+(E)+N_{\mathbf{q}}(T)M_-(E)\}, \quad (3.3)$$

where $N_{\mathbf{q}}(T)$ is the Bose-Einstein distribution function for phonon with energy $\hbar\omega_{\mathbf{q}}$ and $M_\pm$ is given by

$$M_+=\sum_{\lambda_1,s_1}{}'\,[|\langle\lambda s'|\gamma_{\mathbf{q}}|\lambda_1s_1\rangle|^2\delta(E_{\lambda_1}^{s_1}-E_\lambda^s+\hbar\omega_{\mathbf{q}})+|\langle\lambda_1s_1|\gamma_{\mathbf{q}}^\dagger|\lambda s\rangle|^2\delta(E_{\lambda_1}^{s_1}-E_\lambda^{s'}+\hbar\omega_{\mathbf{q}})],$$

$$M_-=\sum_{\lambda_1,s_1}{}'\,[|\langle\lambda s'|\gamma_{\mathbf{q}}^\dagger|\lambda_1s_1\rangle|^2\delta(E_{\lambda_1}^{s_1}-E_\lambda^s-\hbar\omega_{\mathbf{q}})+|\langle\lambda_1s_1|\gamma_{\mathbf{q}}|\lambda s\rangle|^2\delta(E_{\lambda_1}^{s_1}-E_\lambda^{s'}-\hbar\omega_{\mathbf{q}})]. \quad (3.4)$$

Here $\gamma_{\mathbf{q}}$ $[=C(\mathbf{q})\exp(i\mathbf{q}\cdot\mathbf{r})]$ represents the one-electron operator. The phonons couple to the electron via the interaction potential $C(\mathbf{q})$, the form of which depends on the type of interaction. It should be noted that the prime on the summation sign in Eq. (3.4) indicates the exclusion of the diagonal element of $\gamma_{\mathbf{q}}$ and $\Sigma_{\lambda,s}$ represents the triple summations $\Sigma_N\Sigma_{k_y}\Sigma_{k_z}$ of the s valley. Also in Eq. (3.4), the δ-functions express the law of energy conservation in one-phonon collision (emission and absorption) processes, where the effect of the electric field (ICFE) is included exactly through the eigenstate E_λ^s of an electron. The energy-conserving δ functions in Eq. (3.4) imply that when the electron undergoes a collision by absorbing the energy from the field, its energy can only change by an amount equal to the energy of a phonon involved in the transition. This in fact leads to electric-field-induced MPR. In the representation of Eq. (2.2), the matrix elements in Eq. (3.4) are given by

$$|\langle\lambda s|\gamma_{\mathbf{q}}|\lambda's'\rangle|^2=|C(\mathbf{q})|^2K(N,N',u)\delta_{k_x,k_x'+q_x}\delta_{k_z,k_z'+q_z}\delta_{s,s'}, \quad (3.5)$$

where

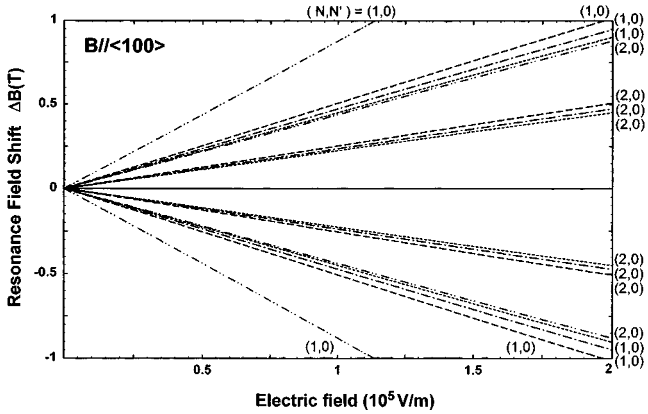

FIG. 1. Resonance field shift of n-Ge for $\mathbf{B}\|\langle 100\rangle$. The quantum number of the Landau level for $m_s^*=0.135$ m is indicated for each line. The dash–double-dotted, dashed, dash-dotted, and dotted lines are for the X_3 point, X_1 point, X_4 point, and Γ point, respectively.

$$K(N,N',u)=\frac{N_n!}{N_m!}\exp(-u)u^{N_m-N_n}[L_{N_n}^{(N_m-N_n)}(u)]^2, \qquad (3.6)$$

with

$$u=(l_B^{s2}/2)[q_y^2+(m_t/m_s^*m_B^s)^2(m_t q_z \sin\theta-m_l q_x \cos\theta)^2]. \quad (3.7)$$

Here $l_B^s=(\hbar/m_t\omega_s)^{1/2}$, $N_n=\min(N,N')$, $N_m=\max(N,N')$, and $L_m^{(n)}(u)$ is the associated Laguerre polynomial.[12]

After some algebra, we obtain from Eqs. (3.4) and (3.5)

$$M_+\approx M_-\approx|C(\mathbf{q})|^2\sum_{N',\pm}K(N,N',u)\,\delta((N'+1/2)\hbar\omega_{s'}-(N+1/2)\hbar\omega_s\pm\hbar\omega_{\mathbf{q}}+\hbar\Delta), \qquad (3.8)$$

where $\hbar\Delta$ is the electric-field-dependent quantities given by

$$\hbar\Delta\equiv(m_t m_l V_d^2/2)(1/m_B^{s'}-1/m_B^s)+eE(y_{\lambda'}^{s'}-y_\lambda^s). \qquad (3.9)$$

To obtain Eq. (3.8) we used the properties

$$\delta(x+a)=\sum_{n=0}^{\infty}(-1)^n(a/x)^n\delta(x)\approx\delta(x) \quad (\text{for } x\gg a). \quad (3.10)$$

Then the relaxation rate (and hence magnetoconductivity) shows, from Eqs. (3.1), (3.3), and (3.8), that the electric-field-induced MPR gives the resonance conditions at

$$(N'+1/2)\hbar\omega_{s'}=(N+1/2)\hbar\omega_s\mp\hbar\omega_{\mathbf{q}}-\hbar\Delta, \qquad (3.11)$$

where N' and $\hbar\omega_{s'}$ $(=\hbar eB/m_{s'}^*)$, respectively, denote the quantum number and the cyclotron energy of the Landau electron of the s' valley, as do N and $\hbar\omega_s$ $(=\hbar eB/m_s^*)$. These peak positions strongly depend on the difference of Landau-level indices, the difference in the effective mass between the initial and final states of the intervalley scattering by phonons, the involved phonon energy, and the strength of the electric field. If we take the limit $E\to 0$ in Eq. (3.11), the last term on the right-hand side in Eq. (3.11) vanishes and the expression gives the hot-electron MPR condition, where the ICFE's are not effective. These for the transverse configuration are same as the theoretical result of Futagawa *et al.*[8] obtained for the longitudinal configuration. In this case, the transition of an electron from the Nth excited state in the s valley to the N'th state of the s' valley, associated with the emission of the phonons, occurs at the resonance magnetic field given by

$$B_{NN'}(0)=\frac{B_{FN}}{N+\alpha_{N'}} \quad (B_{FN}=\omega_{\mathbf{q}}m_s^*/e), \qquad (3.12)$$

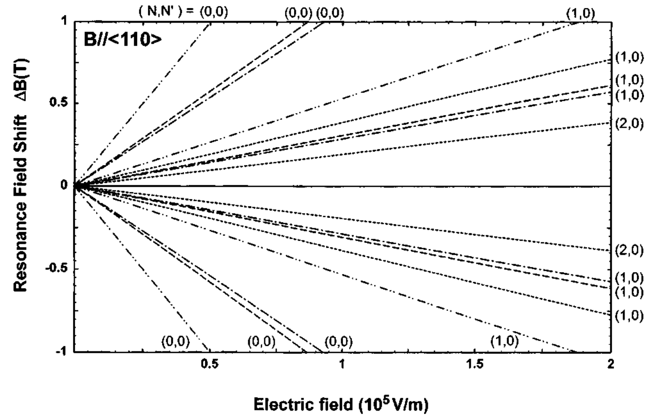

FIG. 2. Resonance field shift of n-Ge for $\mathbf{B}\|\langle 110\rangle$. The quantum number of the Landau level is indicated for each line. The dash–double-dotted, dashed, dash-dotted, and dotted lines are for the X_3 point, X_1 point, X_4 point, and Γ point, respectively. The dotted lines are for $m_s^*=0.099$ m and all the lines except for the dotted lines are for $m_{si}^*=0.099$ m and $m_{sf}^*=0.36$ m, corresponding to the initial and final states of the transition, respectively.

with $\alpha_{N'}=1/2-(N'+1/2)m_s^*/m_{s'}^*$. The MPR conditions for intravalley transition are given by

$$B_{NN'}(0)=B_{FP}/P$$
$$(B_{FP}=\omega_{\mathbf{q}}m_s^*/e, P=N-N'=1,2,3,\ \ldots\ ) \qquad (3.13)$$

if we regard the same cyclotron mass before and after the transitions. In Eq. (3.9), assuming[13] that $y_{\lambda'}^{s'}-y_\lambda^s<0$ or $y_{\lambda'}^{s'}-y_\lambda^s>0$, depending on whether the maximum in the magnetoconductivity appears at magnetic fields $B_{NN'}(E)$ lower or higher than $B_{NN'}(0)$ given by Eq. (3.12), we can make an approximation as $y_{\lambda'}^{s'}-y_\lambda^s\simeq\pm\overline{l}_{B_0'}=\pm(l_{B_0'}^{s'}+l_{B_0'}^s)/2$ with $\overline{l}_{B_0'}\approx(\sqrt{\hbar/m_t eB_0'}/2)(\sqrt{m_s^*}+\sqrt{m_{s'}^*})$ and $B_0'=(2\omega_{\mathbf{q}}/e)(m_s^*m_{s'}^*/|m_{s'}^*-m_s^*|)$. This assumption results in double peaks around the MPR extrema without the ICFE. Equation (3.9) can then be rewritten as

$$\hbar\Delta\equiv(m_t m_l V_d^2/2)(1/m_B^{s'}-1/m_B^s)\pm eE\overline{l}_{B_0'}. \qquad (3.14)$$

Note that we did not perform the calculation of the amplitude of magnetoconductivity oscillation because we are interested in the hot-electron MPR peak positions.

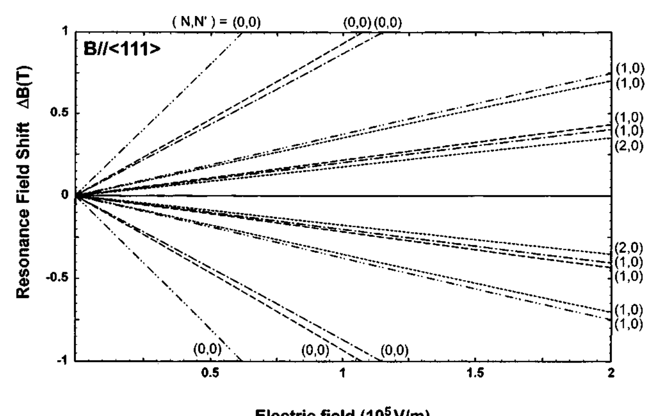

FIG. 3. Resonance field shift of n-Ge for $\mathbf{B}\|\langle 111\rangle$. The quantum number of the Landau level is indicated for each line. The dash–double-dotted, dashed, dash-dotted, and dotted lines are for X_3 point, X_1 point, X_4 point, and Γ point, respectively. The dotted lines are for $m_s^*=0.082$ m and all the lines except for the dotted lines are for $m_{si}^*=0.082$ m and $m_{sf}^*=0.207$ m, corresponding to the initial and final states of the transition, respectively.

IV. RESULTS

In this section we present the numerical results for MPR peak shifts due to the intracollisional field effect, by using Eqs. (3.11)–(3.14), and analyze these results in terms of the strength of the electric field. For n-type Ge, it is known that the conservation of momentum allows electrons to be scattered by the phonons at $\mathbf{\Gamma}$ and $\mathbf{X}$ points.[14] As a result, the possible phonons[15] for n-type Ge are $\mathbf{\Gamma}$ point LO TO (37.7 meV), $\mathbf{X}_4$-point TO (34.2 meV), $\mathbf{X}_1$-point LA LO (29.8 meV), and $\mathbf{X}_3$-point TA (9.93 meV). To visualize the resonance field shifts ΔB associated with the emission of the phonons, we plotted Figs. 1, 2, and 3 corresponding to $\mathbf{B}\|\langle 100\rangle$, $\mathbf{B}\|\langle 110\rangle$ and $\mathbf{B}\|\langle 111\rangle$, respectively, where the dependence of the shifts on the strength of the electric field, the magnetic-field direction, the possible phonon energy, and the difference of Landau-level indices is presented. The shifts ΔB $[\equiv B_{NN'}(E)-B_{NN'}(0)]$ are the difference between the field-induced resonant magnetic field $B_{NN'}(E)$ given by Eqs. (3.11) and (3.14) and the resonant field $B_{NN'}(0)$ given by Eq. (3.12) or (3.13), depending on the type of transitions.

The resonance field shifts of n-Ge in the transverse configuration are presented in Fig. 1 for $\mathbf{B}\|\langle 100\rangle$. The intravalley MPR appears since all the equivalent valleys have an identical effective mass for $\mathbf{B}\|\langle 100\rangle$. As shown in Fig. 1, the shifts increase with decreasing the possible phonon energy, linearly with increasing electric field, and strongly with decreasing the difference of Landau-level indices before and after the intravalley transitions. The splitting of the MPR peak positions take place, which is due to the nonvertical transition at high electric field, as pointed out by Mori *et al.*.[13] The upper and lower parts in the figure correspond to $\Delta y>0$ and $\Delta y<0$, respectively. Accordingly, in the former case, the resonance peak positions are shifted to the higher-magnetic-field side as electric fields are increased and as the possible phonon energy and the difference of Landau-level indices are decreased, while in the latter case, they are shifted to the lower-magnetic-field side as electric fields are increased and as the possible phonon energy and the difference of Landau-level indices are decreased. Note that our results for the limit $E\rightarrow 0$ reduce to the previous results,[16] which agree with the experimental values of Eaves *et al.*[2] and Harper *et al.*[5] for the transverse configuration and with the experimental values of Hamaguchi *et al.*[3,4] for the longitudinal configuration.

Unlike the case of $\mathbf{B}\|\langle 100\rangle$, as can be seen from Figs. 2 and 3, the MPR peaks of the intervalley scattering occur at $\mathbf{X}$ points for $\mathbf{B}\|\langle 110\rangle$ and $\mathbf{B}\|\langle 111\rangle$, due to the difference in the effective mass between the initial and final states. As illustrated in Fig. 1, the shifts increase with decreasing the possible phonon energy, linearly with increasing electric field, and strongly with decreasing the difference of Landau-level indices due to before and after the intervalley transitions occurring at $\mathbf{X}$ points and due to before and after the intravalley transitions occurring at $\mathbf{\Gamma}$ points. Note that in the case of the limit $E\rightarrow 0$, our results occurring at $\mathbf{X}_4$ points for $\mathbf{B}\|\langle 110\rangle$ and $\mathbf{B}\|\langle 111\rangle$ become the previous results,[16] which are in good agreement with the experimental values of Eaves *et al.*[2] and Harper *et al.*[5] for the transverse configuration and with the experimental values of Yamada *et al.*[7] and Futagawa *et al.*[8] for the longitudinal configuration.

It is noted that our results for the relaxation rate and the dc magnetoconductivity are based on the following approximation as $y_{\lambda}^{s'}-y_{\lambda}^{s}\simeq\pm\overline{l}_{B_0'}$ and $\delta(x+a)\approx\delta(x)$ (for $x\gg a$). Furthermore, any analytical expression for the integration over $\mathbf{q}$ of Eq. (3.3) has not been made since we are interested only in the electric-field-induced MPR peak positions.

V. CONCLUSION

In conclusion, we have presented a theory of electric-field-induced MPR in n-Ge for the transverse configuration and obtained the MPR conditions given in Eqs. (3.11) and (3.14). As can be seen from Eqs. (3.11) and (3.14), MPR peak positions for the intervalley scattering by phonons strongly depend on the strength of the electric field, the possible phonon energy, the difference of Landau-level indices, and the magnetic-field direction, which leads to the difference in the effective mass between the initial and final states. According to the nonvertical transition due to the ICFE, double peaks take place. One of the peaks is shifted to the lower-magnetic-field side and the other is shifted to the higher-magnetic-field side as electric fields are increased and as the possible phonon energy and the difference of Landau-level indices are decreased. We expect that our results will help in the qualitative understanding of the physical characteristics of the electric-field-induced MPR effect in materials with the many-valley structure.

ACKNOWLEDGMENTS

This research was supported in part by the Basic Science Research Institute Program, Ministry of Education under Grant No. BSRI-97-2405 and in part by the Korea Science and Engineering Foundation under Grant No. 971-0207-029-2.

[1] R. J. Nicholas, Prog. Quantum Electron. **10**, 1 (1985).
[2] L. Eaves *et al.* (unpublished); L. Eaves *et al.*, J. Phys. C **8**, 1034 (1975).
[3] C. Hamaguchi *et al.*, in *Application of High Magnetic Fields in Semiconductor Physics*, Proceedings of the International Symposium, edited by G. Landwehr (Springer, Berlin, 1983), p. 423.
[4] R. J. Nicholas, Prog. Quantum Electron. **10**, 1 (1985).
[5] P. G. Harper *et al.*, Rep. Prog. Phys. **37**, 1 (1973).
[6] B. K. Ridley, *Quantum Processes in Semiconductors* (Clarendon, Oxford, 1993), p. 316.
[7] K. Yamada *et al.*, Physica B **177**, 461 (1992).
[8] H. Futagawa *et al.*, J. Phys. Soc. Jpn. **62**, 4407 (1993).
[9] D. K. Ferry and C. Jacoboni, *Quantum Transport in Semiconductors* (Plenum, New York, 1992), p. 3.
[10] J. Y. Ryu and S. D. Choi, Phys. Rev. B **44**, 11 328 (1991).
[11] A. Suzuki, Phys. Rev. B **45**, 6731 (1992).
[12] I. S. Gradsteyn and I. M. Ryzhik, *Table of Integrals, Series and Products* (Academic, New York, 1965).
[13] N. Mori *et al.*, J. Phys. Soc. Jpn. **57**, 205 (1988).
[14] R. T. Payne, Phys. Rev. **139**, A570 (1965).
[15] G. Nilsson and G. Nelin, Phys. Rev. B **3**, 364 (1971).
[16] S. C. Lee *et al.*, J. Korean Phys. Soc. **32**, 138 (1998).